Renewable Energy-Based Load Frequency Stabilization of Interconnected Power Systems Using Quasi-Oppositional Dragonfly Algorithm

B. Vedik[1] · Ritesh Kumar[1] · Ram Deshmukh[1] · Sumit Verma[2] · Chandan Kumar Shiva[1]

Abstract
It is already established that the renewable integration effects to the power system are nonzero and become more important with large penetrations. Thereby, the impacts of renewable energy sources (RESs) after integration are studied in this work to stabilize grid frequency of the studied test power system model. Initially, the two-area power system model is studied as the test system. The purpose is to show the tuning efficiency of non-conventional quasi-oppositional dragonfly algorithm (QODA) algorithm as compared to conventional way of tuning technique. It is showed that QODA algorithm is quite effective to find the optimal parameters of proportional–integral–derivative (PID) controller in load frequency control performance. Further, the three-area power system model integrated with RESs is studied. The work done here is to study the impacts of wind turbine generation, solar thermal power generation and solar photovoltaic on system frequency oscillations. The PID controller is employed as the supplementary control task, and its parameters are tuned by QODA algorithm. The integral of time absolute error is chosen as the objective function, and further performance indices are determined at the end of the execution of the program to examine the performance of the designed QODA-based PID controller. Following the integration of RESs, the impacts on frequency deviation through simulation results are also presented. The simulation results showed that the RESs are quite effective in regulating the power system frequency deviation understudied.

Keywords Grid frequency oscillations · Interconnected power system · Optimization · Solar photovoltaic · Solar thermal power generation · Wind turbine generation

List of Symbols

a_{12}	Rated area capacity
B	Frequency bias constant (p.u.MW/Hz)
D	System damping of area (p.u.MW/Hz)
f_{sys}	Nominal system frequency (Hz)
H	Inertia constant (s)
i	Subscript referred to the i-th area ($i = 1, 2, 3$)
K_r	Steam turbine reheat constant
K_p	Power system gain constant
R_{th}, R_h	Governor speed regulation parameter of thermal unit and hydro unit
T_{ij}	Synchronizing coefficient between areas i and j (p.u.)
T_g	Steam governor time constant
T_r	Steam turbine reheat time constant (s)

✉ Chandan Kumar Shiva
    chandankumarshiva@gmail.com

    B. Vedik
    b.vedik@gmail.com

    Ritesh Kumar
    riteshraj3336@gmail.com

    Ram Deshmukh
    ramdeshmukh@gmail.com

    Sumit Verma
    sumitverma1990@yahoo.com

1   Department of Electrical and Electronics Engineering, S R Engineering College, Ananthsagar, Hasanparthy, Warangal, Telangana, India

2   Department of Industrial and Management Engineering, Indian Institute of Technology, Kanpur, Uttar Pradesh, India

T_w	Starting time of water in penstock (s)
T_p	Power system time constant
T_t	Steam turbine time constant
K_{de}, K_{pe}, K_{ie}	Electric governor derivative, proportional and integral gains, respectively
ΔP_d	Change in load demand
Δf	Frequency deviation (p.u. Hz)
ΔP_{tie}	Incremental tie-line power deviation (p.u.MW)

Abbreviations

DA	Dragonfly algorithm
GA	Genetic algorithm
ISE	Integral of square error
ITAE	Integral of time absolute error
ITSE	Integral of time square error
IAE	Integral of absolute error
LFC	Load frequency control
PID	Proportional–integral–derivative
PV	Photovoltaic
QODA	Quasi-oppositional Dragonfly algorithm
RESs	Renewable energy sources
SLP	Step load perturbation
STPG	Solar thermal power generation
WTG	Wind turbine generator
ZN	Ziegler–Nichols

1 Introduction

1.1 General

In an interconnected power system, frequency stability is one of the important issues for power system operators (Bevrani et al. 2010). The appearance of frequency oscillations within the system is an indication of an unbalance between generation and load demand, which need to be controlled (Karavas et al. 2015). In the power system study, the electrical loads change frequently that cannot be uncontrolled; therefore, the load frequency control (LFC) becomes a significant tool for the satisfactory performance of the power system. With the restructuring of the power system and the incorporation of renewable energy sources (RESs), the system behavior study becomes important in view of proper operation and control. The changed power system structure comes with the higher randomness and uncertainty in the active power generation. A higher RESs penetration in the power system increases uncertainties at the time of abnormal operation and brings various technical difficulties that need to be studied (Torreglosa et al. 2014).

1.2 Literature Review

The addition of RESs to the conventional power system and their effects has been studied in this section subjected to preceding work done. It has been observed that the dynamic behavior of the multi-agent hybrid power system after the addition of RESs behaved in a different way than that of the thermal power system (Karavas et al. 2015). The other points of observations are the penetration of RESs into the power grid may escalate uncertainties during abnormal operation, brings in various technological implications and elevated numerous queries on the operation of conventional power system control methods in the new environment. An important feature of RESs is their fast active power injection to support frequency regulation has been discussed by Bevrani et al. (2010). Following a power mismatch between generation and load demand, the active power produced by these RES swiftly improves the power system frequency. The more effect is observed during a change in the load that lasts for few seconds; traditional generating units should ultimately compensate the power balance by shifting their active power injection/generation (Mauricio et al. 2009). As the transformed power system requires reliable integration of large and various types of generation units into the power grid, a substantial effort is required to accommodate and efficiently accomplish these unique planning and operating characteristics (Slootweg and Kling 2003). An adaptive deadbeat controller has been developed by Muhssin et al. (2017) for the sake of rapid frequency response. In recent studies, the impacts of wind turbine generators (WTGs) on system dynamics for frequency deviation control have been presented by Rosas (2004). The stored kinetic energy of WTG due to inertia property in primary frequency control has been studied by (Morren et al. 2006). In other work, the tie-line power flow control for small frequency oscillation with wind power has been presented by Slootweg and Kling (2003). The wind farm contribution in improving frequency control during the integration of the power grid has been discussed by Tavakoli et al. (2018). To boost system frequency characteristics, the impacts of redox flow batteries and then optimized proportional–integral–derivative (PID) controller have been studied by Kouba et al. (2016). A comparative study of genetic algorithm (GA) and particle swarm optimization method as a better optimization technique in the case of a single-area test system has been reported by Modi et al. (2013). The wind power penetration of wind farm with three thermal units equipped with LFC has been addressed by Luo et al. (2007). The LFC study of power system involving thermal-, hydro- and gas-based generating units in the presence of wind power plant under different operating modes and penetration level has been studied by Aziz et al. (2018).

To achieve clean energy, other RESs like solar thermal power generation (STPG) and solar photovoltaic (PV) gener-

ating units may be integrated in the power system dynamics. The impacts of dish-stirling solar thermal system for LFC study of an unequal two-area thermal power system have been studied by Rahman et al. (2016). In this work, the thermal systems are equipped with reheat turbine, generation rate constraint (GRC) and governor dead band. The effects of PV on system frequency response characteristics have been reported by Yan et al. (2015). The working of PV system in primary load frequency characteristic in different operating conditions has been considered by Tavakkoli et al. (2018). A comprehensive supervisory control of a hybrid system consists of wind and PV generation subsystems, and a battery bank has been studied by Valenciaga and Puleston (2005). A study of autonomous hybrid power generation systems consisting of WTGs, STPG and solar PV subjected to alleviate the system frequency deviation for different configurations of hybrid power system has been discussed by Das et al. (2012).

The above discussions showed the application of wind power system, STPG and PV system in the frequency control problem. Hence, there is still scope of research in the area of LFC with the integration of these RESs into interconnected power system. Further, from the literature survey it has been identified that evolutionary techniques can be utilized for the enhancement of RESs control strategy-based interconnected power system. However, trapping into local optima, less exploration capabilities, premature convergence and high computational time are some of problems connected with the studied evolutionary optimization techniques (Shayeghi et al. 2007). This has made the prospect of employing new optimization methods for the significant enhancement in load subsequent performance by optimal tuning of controller gains. The present work done utilizes a quasi-oppositional dragonfly algorithm (DA) (QODA) algorithm to optimize the controller gains installed in the studied power system model for the substantial improvement in LFC performance. The impacts of this algorithm may be understand in terms of its diversities in applications such as machine learning, neural network, image processing, robotics and engineering. The other significance is that DA can be easily modified, hybridized and applied in various applications (Meraihi et al. 2020). QODA with high exploration and exploitation capabilities due to unique swarm behavior and quasi-oppositional-based learning concept has an ability to identify the promising region of the solution space with fast convergence rate and less mathematical computation. This technique provides reliable and competitive results when compared to other well-known nature-inspired methods (Nandi et al. 2017; Shiva and Mukherjee 2015, 2016). The system dynamic response is compared with GA and the conventional way of tuning PID controller. For a comprehensive evaluation of QODA performance, the conventional way of tuning PID controllers is used as a baseline.

1.3 Motivation of this Work

Due to the integration of RESs to the system dynamics, the modern power systems are under the transition phase and faced lots of new challenging issues to study LFC problem (Modi et al. 2013). With larger penetration of RESs to the power system decreases the overall inertial response ability of the system. By introducing an additional supplementary control mechanism, the inertial response capability of the system may be restored (Morren et al. 2006). The effects of RESs may be considered as a power sources with the capability of rapid control of primary frequency control. As per the fast development of RESs, it has been tried to integrate with conventional power systems. Presently, renewable energy sources such as wind power, solar PV systems and STPG are the most promising and most utilized technologies for integrating into the power system. However, with an increase in size and number of RESs, the stability issues due to the interaction of RESs with power system when compared to other conventional power system have been studies in Ullah et al. (2008). Therefore, new control strategies are required to perform frequency stability analysis with the integration of large RESs during power system operation. Based on the work in the literature, it is required to design effective controllers so as to achieve better frequency regulation for the interconnected power system model incorporated with RESs. In view of this, in this work, the powerful QODA is addressed for the tuning task.

1.4 Contribution of this Article

This paper covers the issues concerning the impacts of RESs on frequency regulation perspective. Also, an effective QODA algorithm-based optimized PID controller is proposed to regulate the frequency deviations in the studied test system. The effectiveness of the proposed approach is showed through a comparative study of the dynamic responses. The contribution of this article may be summarized as follows

(a) The tuning efficiency of QODA algorithm is compared to conventional way of tuning control techniques for the studied two-area power system model.
(b) LFC study of the interconnected three-area power system model is studied with the impacts of RESs.
(c) The LFC dynamic performance analysis is carried out with and without RESs.

The present work integrates the RESs to traditional generating units for the load frequency control study. For this, a suitable dynamic model is designed such that it considers the uncertainties and the non-linearities in the power system. In this study, a three-area hydrothermal power system

model is considered with the integration of RESs. The rest of the article is structured as follows. A short description on the studied interconnected power system model and the control technique is stated in Sect. 2. Section 3 details the optimization task process for the present problem. A brief overview on the implemented QODA technique is shown in Sect. 4. Section 5 shows some fine observations for the presented simulation-based results. Lastly, Sect. 6 concludes the outcomes of the resultant pieces.

2 System Configuration and Characteristics

2.1 WTG: Basic Concept

The simplified model of a WTG by first-order transfer function $\left(G_{\text{wtg}}(s)\right)$ may be given in (1) (Lee and Wang 2008; Singh et al. 2013)

$$G_{\text{wtg}}(s) = \frac{P_{\text{wtg}}}{P_{\text{w}}} = \frac{K_{\text{wtg}}}{1 + s\,T_{\text{wtg}}} \tag{1}$$

where K_{wtg} is the gain constant and T_{wtg} is the time constant of the WTG.

2.2 STPG: Basic Concept

The transfer function of STPG $\left(G_{\text{stpg}}(s)\right)$ may be shown in (2) (Shankar and Mukherjee 2016).

$$G_{\text{stpg}}(s) = \frac{P_{\text{stpg}}}{P_{\text{sol}}} = \frac{K_{\text{t}}}{1 + s\,T_{\text{t}}} \frac{K_{\text{s}}}{1 + s\,T_{\text{s}}} \tag{2}$$

where K_{t} and K_{s} are the gain constants and T_{t} and T_{s} is the time constants of the STPG.

2.3 PV: Basic Concept

PV cell is an electrical device that produces electrical power when exposed to sunlight. The generated power is connected to a suitable load. With a decrease in the cost of the system (such as DC/AC inverters, manpower, PV modules, fittings, and cables), PV technology has the potential to become one of the key RESs for electricity supply in the future (Pan and Das 2015). For low-frequency domain analysis, the transfer function model of PV system $\left(G_{\text{pv}}(s)\right)$ may be shown in (3) (Nayeripour et al. 2011)

$$G_{\text{pv}}(s) = \frac{P_{\text{pv}}}{P_{\phi}} = \frac{1}{1 + s\,T_{\text{pv}}} \tag{3}$$

where T_{pv} is termed as time constant of the PV.

2.4 Supplementary Controller

The PID secondary controller is used to maintain the power flow between the interconnected areas at scheduled values and also to control the synchronous generators to provide a secondary response, which is always delayed at a certain amount of time after the primary response. It is employed in the feedback path to maintain the desirable performance of the studied test system. The transfer function of the PID controller of i-th area $\left(K_{\text{pid}i}(s)\right)$ may be stated in (4) (Pal and Dey 2015).

$$K_{\text{pid}i}(s) = \frac{u_i}{\text{ACE}_i} = K_{pi} + \frac{K_{ii}}{s} + s\,K_{\text{d}i} \tag{4}$$

In (4), K_p, K_i, K_i are the proportional, integral and derivative gains, respectively. Also u_i, ACE_i are the controlled output and tracking error signal of i-th area.

2.5 Studied Power System Model

Figure 1 depicts the studied two-area power system model with non-reheat turbine (Shiva et al. 2015). The plant for the power system comprises of the power system block, governor and turbine. All the parameters of this system are shown in "Appendix" section. This model is taken for showing the tuning efficiency of the QODA algorithm in comparison with both conventional and non-conventional ways of tuning PID controller as well as showing the output powers of synchronous generators.

In further investigation, the studied test system is a three-area hydrothermal power system model having two reheats thermal unit and one hydrounit with PID controller in each area. Each area of the test system consists of speed governing system, turbine and generator. Area-1 and area-2 are reheated thermal power generating system while area-3 is hydrounit. Each area has a rating of 2000 MW with a nominal load of 1000 MW. The typical value of for hydro plant is considered to be relatively much higher (typical value of GRC being 270%/min (0.0045 p.u.MW/s) for upper generation limit and 360%/min (0.06 p.u.MW/s) for lower generation limit as compared to 3%/min (0.0005 p.u.MW/s) for reheat thermal unit. The studied three-area power system model is integrated with RESs. In this model, the RESs are integrated in two different prospects. In the first prospect, area-1 is integrated with WTG, area-2 is integrated with STPG, and area-3 is integrated with PV for the three-area power system model. In this model, multiple-step load perturbation (SLP) is applied to the system (refer Fig. 2). In the second one, only area-1 is integrated with WTG for the three-area power system model subjected to random SLP (refer Fig. 3). Corresponding to this, the structure of RESs used is shown in Fig. 4.
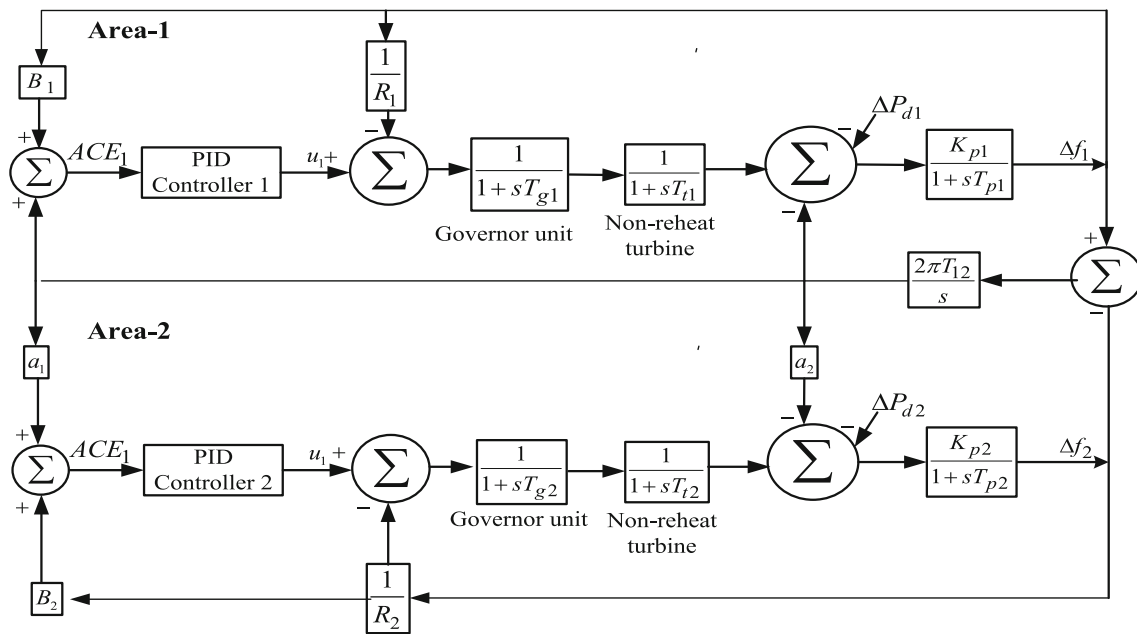
Fig. 1 Block diagram representation of two-area non-reheat thermal power system model (Shiva et al. 2015)
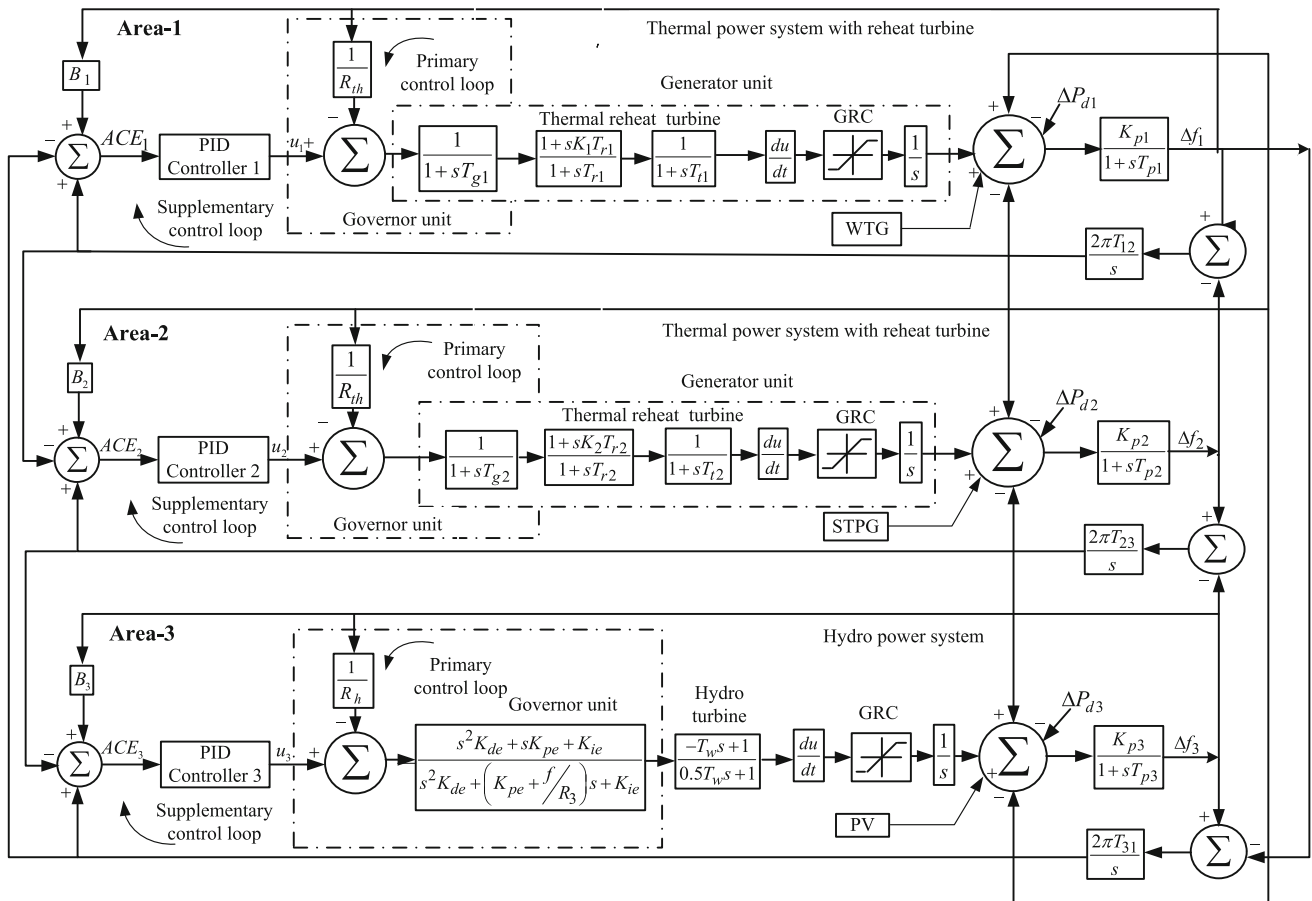

Fig. 2 Block diagram representation of three-area hydrothermal power system model with RESs. Scenario (I): WTG connected to area-1. STPG is connected to area-2. PV connected to area-3
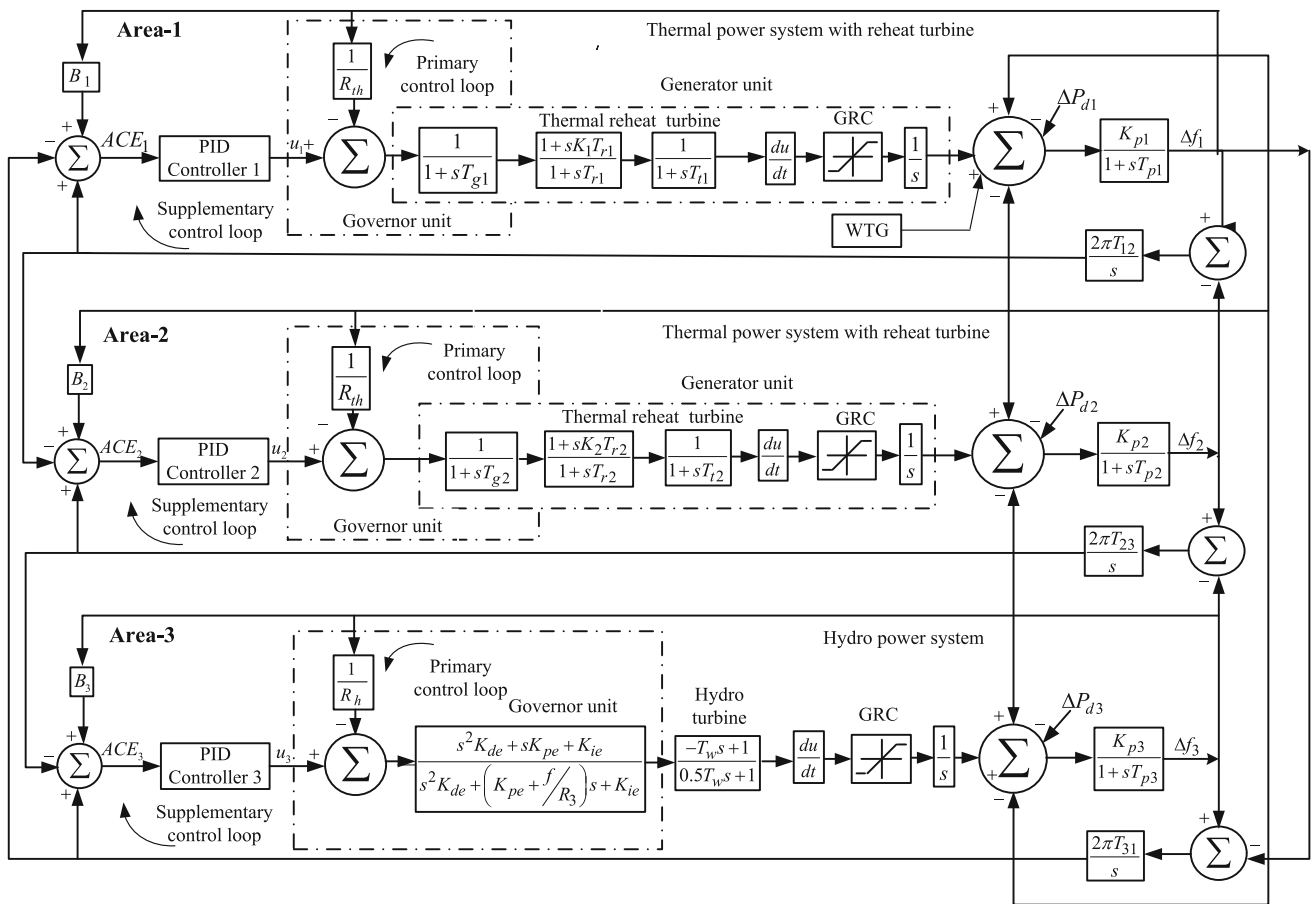
Fig. 3 Block diagram representation of three-area hydrothermal power system model with WTG. Scenario (III) WTG connected to area-1

3 Optimization Problem Formulation

The tuning of a PID controller gains for optimal control of a plant (process) depends on the plant's behavior. To design the PID controller, an engineer must select the tuning approach of design gains to enhance the transient response and steady-state error. Further, the desired response for the step response of the closed loop system should consist of minimal settling time with a small or no overshoot (Farahani et al. 2012).

3.1 Choice of the Objective Function

The purpose of the simulation is to show the efficacy, potentiality and controllability of the proposed QODA algorithm over GA and the conventional way of tuning PID controller gains in LFC problem. In response to this, an objective function is defined. According to the control system theory, an objective function may be defined in terms of integral of time multiplied squared error (ITSE), integral of absolute error (IAE), integral of time multiplied absolute error (ITAE) and integral of squared error (ISE). ISE integrates the square of the error over time; hence, large errors are affected when compared to the smaller ones. As IAE gives significance to

only absolute error and ITSE penalizes squared error, these conditions are not often used as the objective function in controller design. ITAE criterion integrates the absolute error multiplied by the time and penalizes errors that exist after a long time much more heavily than at the start of the response. The other point is, in order to reduce the weighting of the large initial error and to penalize the small errors occurring later in the response more heavily, ITAE may be used. The ITAE produces smaller overshoots and oscillations than the IAE and ISE indices. ITAE tuning produces systems which settle much more quickly than ISE. In addition, it is the most sensitive of the three, i.e., it has the best selectivity and is a better choice. It has been reported that ITAE is a better objective function in LFC studies (Shabani et al. 2013). The expression for ITAE may be stated in (5).

$$\text{ITAE} = \int_0^{t_{\text{sim}}} \left\{ |\Delta f_i| + \left| \Delta P_{\text{tie}ij} \right| \right\} t \, dt \tag{5}$$

In (5), t_{sim} is the simulation time (in s), Δf_i is frequency deviation of i-th area and $\Delta P_{\text{tie}ij}$ is the tie-line power deviation between area-i and area-j.
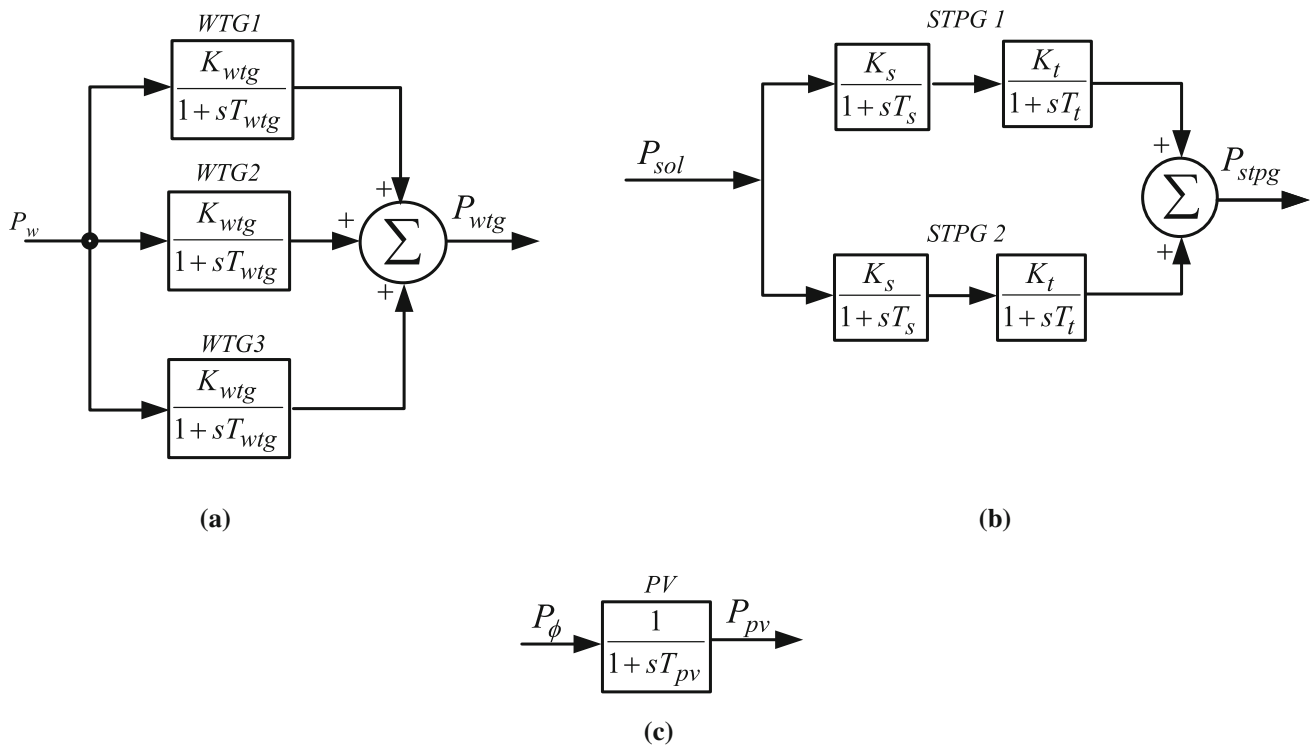
Fig. 4 Structure of the RESs to be applied: **a** WTG, **b** STPG and **c** PV generation

3.2 Constrained Optimization

The constraints for the optimization task are the PID controller gains K_p, K_i, K_d whose true approximate values are to be determined within the superscript min and max representing the minimum and the maximum values. Here, the LFC optimization problem is solved by QODA algorithm to minimize the ITAE to obtain the optimal parameters of the controllers subject to the following constraints. The limits of the constraints may be defined in (6).

$$K_{pi}^{min} \leq K_{pi} \leq K_{pi}^{max}$$
$$K_{ii}^{min} \leq K_{ii} \leq K_{ii}^{max} \tag{6}$$
$$K_{di}^{min} \leq K_{di} \leq K_{di}^{max}$$

where i denotes the area.

In the optimization process, convergence speed to obtain the optimal solution more or less depends upon the unknown system parameters. Initially, the maximum and minimum range of parameters is unknown. Therefore, the program is executed by considering a wider solution range of parameters. After executing the program for number of times the shorter range of unknown parameters is identified such the solution of the problem is met. After identifying of the solution space, the proposed algorithm is executed and the best optimal solution obtained is selected as the controller param-

eters. The maximum and minimum range of controller gains lies within 0.001–1.

3.3 Measure of Performance

The present prospect is on the mathematical formulation to design the optimal gains of the PID controllers. In view of this, in addition to the objective function defined in (8), the performance indices like IAE, ITSE and ISE are also calculated to show the tuning consistency of the designed QODA-based PID controller. These three may be stated by (7)–(9), in order.

$$IAE = \int_0^{t_{sim}} \left\{ |\Delta f_i| + |\Delta P_{tieij}| \right\} \, dt \tag{7}$$

$$ITSE = \int_0^{t_{sim}} \left\{ (\Delta f)^2 + (\Delta P_{tieij})^2 \right\} t \, dt \tag{8}$$

$$ISE = \int_0^{t_{sim}} \left\{ (\Delta f)^2 + (\Delta P_{tieij})^2 \right\} \, dt \tag{9}$$

The values of these performance indices are computed at the end of the execution of proposed method.

4 Applied Optimization Techniques

The optimization technique is quite essential for the optimal design of the dynamic controller. The better the designed controller gives better dynamic performance of the power system under study.

4.1 Dragonfly Algorithm

The dragonfly algorithm (DA) is a swarm-based technique that mimics the behavior of swarms and is proposed by Mirjalili (2016) in the year 2015. These dragonflies are regarded as small predators, which hunt the small insects or preys such as mosquitoes and butterflies. Unlike other swarms, these dragonflies have two unique swarming behaviors, namely migrating (also known as dynamic swarm) and hunting (also known as static swarm). In dynamic swarm, large numbers of dragonflies form a single group to migrate over long distances in one direction. In static swarm behavior, the large numbers of dragonflies scattered into small groups over a small area to hunt the preys. In this phase, the dragonflies in search of food perform local movements with sudden changes in the flying path. These are the two main features of the static swarms, i.e., static and dynamic swarming dragonflies' behavior. The above-mentioned two unique swarm behaviors form the main inspiration in developing new metaheuristic dragonfly optimization technique. The static and dynamic behavior of dragonflies is analogous to the exploration and exploitation phases of evolutionary techniques, respectively. Thus, in the optimization process position of each dragonfly denotes a solution in the search space (Mirjalili 2016).

To direct the dragonflies to various directions, three primitive principles of swam behavior have been considered according to Reynolds (1987). These three principles include:

(a) Separation: This principle involves avoiding the static collision between individuals (dragonflies).
(b) Alignment: This principle specifies the matching of individual dragonfly velocity with the neighboring individuals (dragonflies).
(c) Cohesion: This principle pertains to the inclination of individuals (dragonflies) toward the center of the mass of the neighborhood.

In addition to the above-mentioned principles, two additional principles for survival of swarms, namely attraction toward the prey and diversion from the enemies, are considered. Therefore, the positions of dragonflies are updated by taking into account of five principles stated above and are mathematically modeled as follows.

The separation between the individual dragonflies is calculated using (10) (Mirjalili 2016)

$$S_i = -\sum_{j=1}^{N} X - X_j \qquad (10)$$

where X indicates the current individual position, X_j denotes the position of neighboring j^{th} individual and N represents the number of dragonflies (neighboring individuals).

Alignment between the individuals is calculated using (11) (Mirjalili 2016):

$$A_i = \frac{\sum_{j=1}^{N} V_j}{N} \qquad (11)$$

where V_j denotes the velocity of neighboring jth dragonfly.

Cohesion of the ith dragonfly is calculated using (12) (Mirjalili 2016)

$$C_i = \frac{\sum_{j=1}^{N} X_j}{N} - X \qquad (12)$$

where X indicates the current individual position.

Attraction toward a prey is computed using (13) (Mirjalili 2016)

$$F_i = X^+ - X \qquad (13)$$

where X^+ indicates the food source/prey position. In dragonfly algorithm, the best fittest position of dragonfly is considered as the position of food source (Mirjalili 2016).

Diversion from the enemies is computed as:

$$E_i = X^- + X \qquad (14)$$

where X^- represents the enemy position. In the present algorithm, the worst fittest position of dragonfly is considered as the position of enemy.

To stimulate the movement of dragonflies, the position is updated using the step vector ΔX. This step vector ΔX is modeled by utilizing the five corrective patterns and is computed as follows (Mirjalili 2016).

$$\Delta X_{t+1} = (s S_i + a A_i + c C_i + f F_i + e E_i) + w \Delta X_t \qquad (15)$$

where $s, a, c, f,$ and e represents the separation weight, alignment weight, cohesion weight, food factor and enemy factor, respectively. S_i denotes the separation of the ith individual dragonfly, A_i represents the ith individual dragonfly, C_i indicates the cohesion of the ith individual dragonfly, F_i symbolizes the food source of the ith individual dragonfly, E_i

denotes the enemy position of the ith individual dragonfly, w represents the inertia weight, and t specifies the iteration counter (Mirjalili 2016).

The five weights, namely s, a, c, f, and e, play a major role in directing the artificial dragonflies toward the food source. In order to explore the food source for a given search space, high alignment and low cohesion weights are assigned. However, in order to exploit the identified food source, low alignment and high cohesion weights are used. Therefore, for transition from exploration to exploitation the radii of the neighborhoods dragonflies are proportionally increased with iteration count. Further, to balance the exploration and exploitation the swarm factors are adaptively tuned during optimization process (Mirjalili 2016).

The positions of dragonflies are updated using (16a) if at least one neighboring dragonfly is available; otherwise, the artificial dragonflies perform random walk (Levy flight) around the search region to enhance the randomness and stochastic behavior using (16b) (Mirjalili 2016).

$$X_{t+1} = X_t + \Delta X_{t+1} \tag{16a}$$

$$X_{t+1} = X_t + \text{Levy(d)} \times X_t$$
$$\text{Levy}(x) = 0.01 \times \frac{\text{rand}_1 \times \sigma}{|\text{rand}_2|^{\frac{1}{1.5}}} \tag{16b}$$

However, it is found in literature (Rahman and Rashid 2019) the correlation between the position updating of dragonflies and centroid of the population is less. Due to this, the DA suffers from finding the global optimal solution and finally gets trapped into local optima. Lastly, this results in less accuracy of the solution. Hence, in order to overcome these drawbacks, a novel QODA is proposed by incorporating the concept of quasi oppositional-based learning to conventional dragonfly algorithm.

4.2 Quasi-Opposition: A Concept

The concept of opposition-based learning (OBL) is introduced in the year 2005 by Tizhoosh (2005). The main aim of this OBL concept is to enhance the accuracy of the solution and accelerate the convergence speed to find global solution. In OBL, an opposite atom (population) is generated simultaneously for each atom (population) in the current population to provide better candidate solution. In the literature (Guha et al. 2017), it has been proved that creating an opposite candidate solution enhances the probability of producing better candidate solution and getting closer to the global optimum solution when compared to creating a random candidate solution. This opposite candidate solution is created by taking the mirror position of the current population (Guha et al. 2017). The procedure to obtain opposite candidate solution is clearly explained using the following two main attributes:

4.2.1 Opposite Number

Opposite number is defined as the mirror point of the current candidate solution from the centre of the search space. For example, let X be a real number defined in an interval $\left[X^{\min}, X^{\max}\right]$, then corresponding opposite number (OX) is generated mathematically by (17) (Rahnamayan et al. 2008)

$$OX = X^{\min} + X^{\max} - X \tag{17}$$

where $X^{\min}$ and $X^{\max}$ are the minimum and maximum limits of X in the search space. Similarly, this definition can be extended to higher dimensions, which is explained as follows.

If $X(X_1, X_2, \ldots X_i \ldots, X_d)$ is a d-dimensional space vector consisting of d-real numbers whose minimum and maximum limits are $X_j = [X_j^{\min}, X_j^{\max}] \forall j \in \{1, 2, \ldots, d\}$. Its opposite vector $OX(OX_1, OX_2, \ldots, OX_d)$ is generated by (18) (Rahnamayan et al. 2008).

$$OX_j = X_j^{\min} + X_j^{\max} - X_j \tag{18}$$

Later, it has been proved mathematically that quasi-opposition number is more likely to produce much closer to global optimal solution than the opposite number is. Thus, the concept of OBL is extended to quasi-oppositional-based learning (QOBL) (Shiva et al. 2015). The concept of QOBL is explained in the next sub-section.

4.2.2 Quasi-Opposite Number

Quasi-opposite number is defined as the process of generating a number between the centre of the search region $\frac{\left(X_j^{\min}+X_j^{\max}\right)}{2}$ and the opposite number $\left(OX_j\right)$. Mathematically, it is defined using (19) (Shiva et al. 2015).

$$QOX_j = \text{rand}\left(\frac{X_j^{\min} + X_j^{\max}}{2}, X_j^{\min} + X_j^{\max} - X_j\right) \tag{19}$$

The pseudo-code of QOBL is given below (Shiva et al. 2015).

$$\text{Co} = (X_j^{\min} + X_j^{\max})/2;$$
$$if \ (OX < Co)$$
$$\quad QOX = Co + (OX - Co) * \text{rand}_1;$$
$$else$$
$$\quad QOX = OX + (Co - OX) * \text{rand}_1;$$
$$end$$

4.2.3 Quasi-Oppositional Population Initialization

The concept of QOBL is useful to provide better starting candidate solutions in the absence of priori knowledge of solutions. The following scheme is utilized to create best fittest solutions using QOBL.

(a)   By initializing the population X of size N randomly within the search space,
(a)   Generate quasi-opposite population (QOX_0) using the concept explained above and
(c)   Finally, select the N fittest candidate solutions from $\{X \cup QOX\}$ as population for each iteration count.

The steps of the QODA-based PID controllers are performed in the following way.

ZN method, the schematic and practical way of tuning of PID control loop becomes possible. It also showed improved dynamic performance and acceptable responses. The advantage of ZN method is it's easy to design. The following advantages of ZN method enforce to use in this work are as follows (Van der Zalm 2004):

(a)   Fine tuning is needed.
(b)   Controller settings are sensitive, resulting in large overshoot and oscillatory responses.
(c)   Poor performance for processes with a dominant delay.
(d)   Very sensitive to parameter variations.
(e)   Parameters of the step response may be hard to determine due to measurement noise.

Algorithm 1: Pseudo code for QODA

Step. 1.   Generate the dragonflies population $X_i (i = 1, 2, ...N)$ with in the specified range of PID-control parameters K_p, K_i, K_d.

Step. 2.   Initialize the step vector $\Delta X_i (i = 1, 2, ...N)$

Step. 3.   While the termination criteria is not achieved
Step. 4.   Calculate the objective function ITAE value for each dragonflies position
Step. 5.   For each dragonfly the quasi-opposition based learning (QOX) is performed using (17) – (19)
Step. 6.   Calculate the objective function ITAE value for each quasi-opposition dragonflies position (QOX)
Step. 7.   Select best N dragonflies position using objective function values obtained in **Step 4** and **Step 6**
Step. 8.   Update the food source position X_f and enemy positions X_e
Step. 9.   Update the five weight factors, namely, s, a, c, f, and e as given in the Appendix section
Step. 10.   Calculate S, A, C, F, and E for each dragonfly using (10)-(14)
Step. 11.   Update the radius of neighboring dragonflies
Step. 12.   *if* at-least one neighboring dragonfly is present for current dragonfly
Step. 13.   Update the velocity and position of current dragonfly using (15) and (16a)
Step. 14.   else
Step. 15.   Update the position vector using (16b)
Step. 16.   endif
Step. 17.   Verify and adjust the new positions of the dragonflies based on the boundary conditions of variables
Step. 18.   end while

4.3 Ziegler–Nichols Step Response Method

For the control system engineers, the time domain-based Ziegler–Nichols (ZN) tuning method has large impacts in determination of PID-based feedback control system. Even due to the known behavior of PID control, it was very difficult to use because of stability concern. With the development of

5 Simulation Results and Analysis

In this section, the simulation results are shown and the impacts of the results are discussed to demonstrate the effectiveness of the proposed QODA technique in load frequency stabilization of the studied test systems with and without the impacts of RESs. In this work, the QODA algorithm
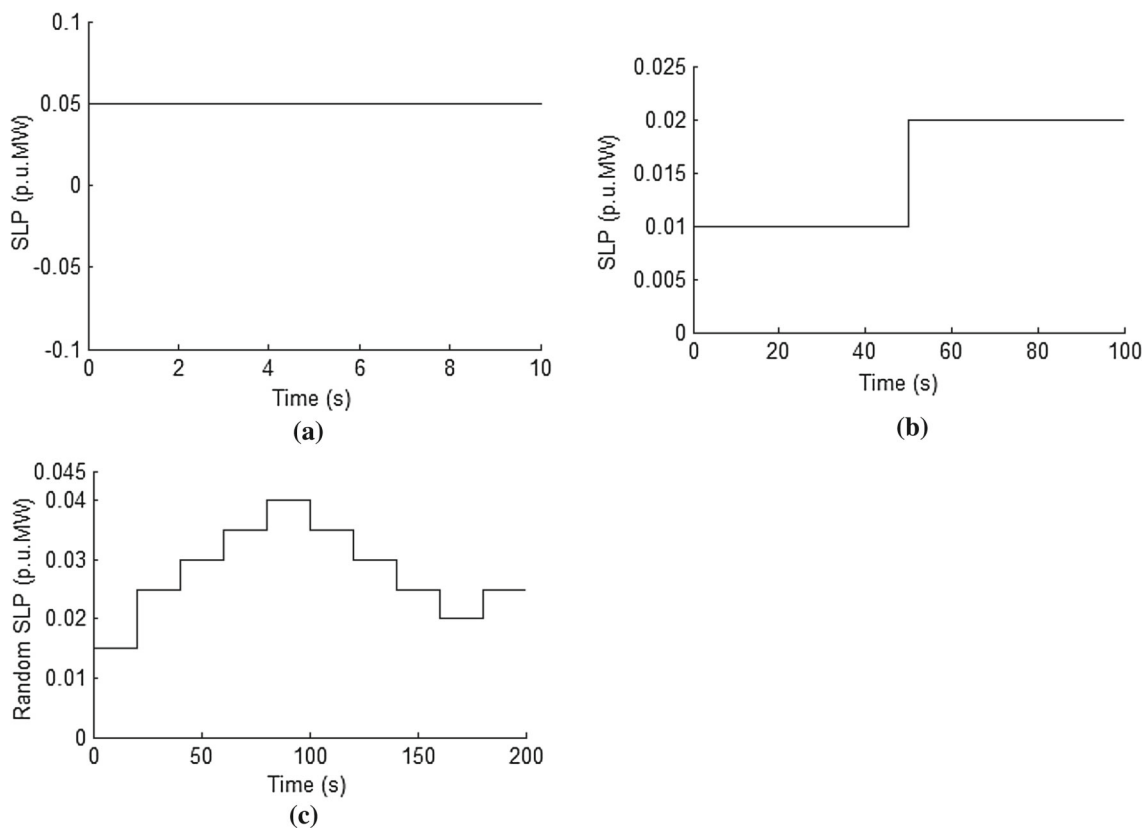
Fig. 5 Studied load perturbation profiles: **a** SLP, **b** multiple SLP and **c** random SLP

Table 1 Optimized PID controller gains for the studied two-area test system (refer Scenario I)

Control area	QODA [proposed]			ZN (Ali and Abd-Elazim 2013)		
	K_p (-ve)	K_i (-ve)	K_d (-ve)	K_p (-ve)	K_i (-ve)	K_d (-ve)
Area-1	1.0	0.7946	0.3923	0.5865	0.5100	0.1686
Area-2	0.6696	0.0115	0.4604	0.5865	0.5100	0.1686

is used. The applications and tuning capabilities of the QODA algorithm are already shown in the previous sections. The QODA algorithm is parameters depended algorithms. Once its parameters are determined, they show improved results. The parameters of the QODA algorithm are shown in "Appendix" section. The presented simulation results are the solutions taken after twenty independent runs of each algorithm. The studied load profiles are presented in Fig. 5. The results of interest are bold faced in the respective tables. The simulation results may be explained as follows. The simulation procedure may be divided into three scenarios as follows:

- Tuning efficiency of QODA algorithm with both conventional and non-conventional methods
- Dynamic responses of three-area power system model with multiple SLP
- Dynamic responses of three-area power system model with random SLP

Table 2 Comparative ITAE and performance indices values for the studied two-area test system (refer Scenario I)

Studied techniques	Objective function	Performance indices		
	ITAE	IAE	ITSE	ISE
ZN [studied]	0.5407	0.2827	0.0126	0.01306
QODA [proposed]	**0.2104**	**0.2073**	**0.0096**	**0.0114**

5.1 Scenario (I): Tuning Efficiency of QODA Algorithm with Both Conventional and Non-conventional Methods

The purpose of this study is to show the comparative analysis of proposed QODA algorithm with the ZN method as the baseline. This is studied on two-area non-reheat power system model (refer Fig. 1). The optimized controller gains
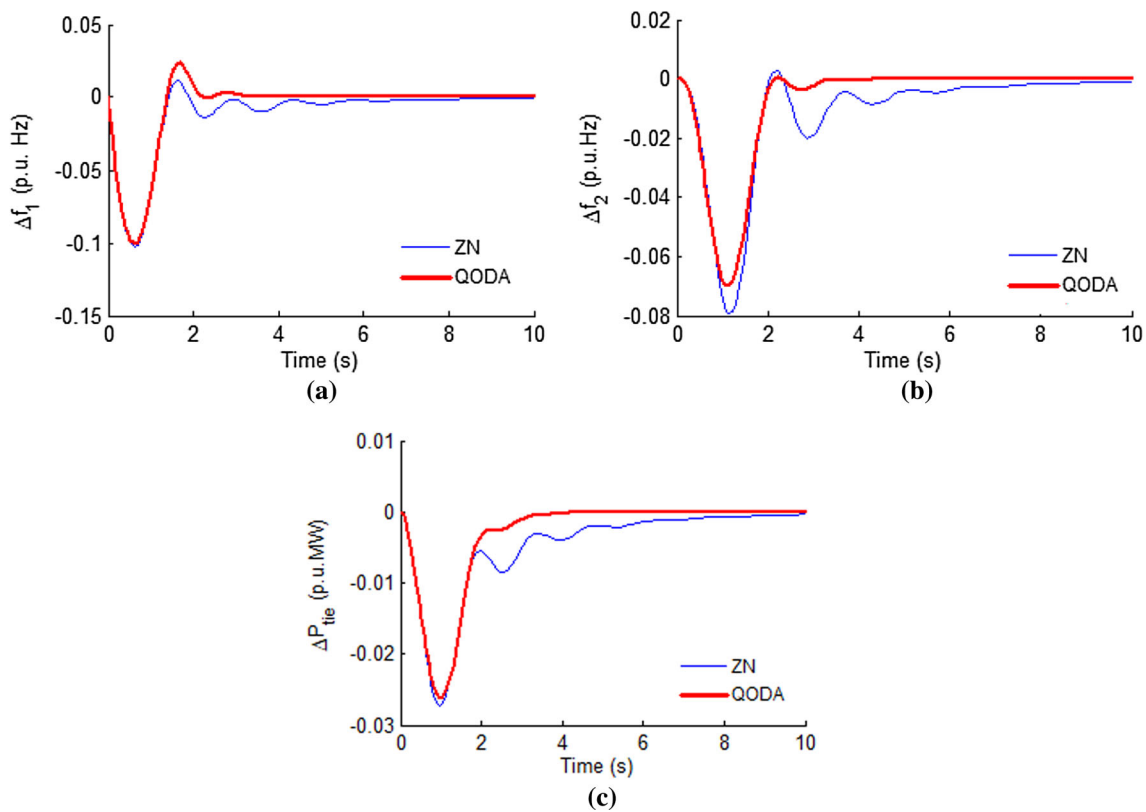
Fig. 6 Comparative dynamic response profiles offered by the studied two-area test system subjected to SLP applied in area-1: **a** Δf_1, **b** Δf_2 and **c** ΔP_{tie}

and performance indices values are shown in Tables 1 and 2, respectively. Table 2 shows the values of ITAE, IAE, ITSE and ISE are less as matched to ZN (Ali and Abd-Elazim 2013). For the dynamic performance analysis, SLP of 0.05 p.u. is applied at $t = 0$ s in area-1 (refer Fig. 5a). The performance characteristics (i.e. Δf_1, Δf_2 and ΔP_{tie} presented in Fig. 6) showed that QODA is a better technique for LFC task as compared to ZN.

However, the optimization and design of PID controller have a direct impact on the behavior of synchronous generators. Thereby, the output powers of synchronous generators in comparison with both GA and QODA algorithms are shown in Fig. 7. The simulation results show that QODA-based design controller controls effectively the output powers of synchronous generators with low oscillations of damping and reached the steady state as fast as compared to GA.

5.2 Scenario (II): Dynamic Responses of Three-Area Power System Model with Multiple SLP

The system dynamic responses are evaluated considering 50% loading with SLP refer Fig. 5b applied in area-1. The system is incorporated with PID controller separately as secondary controller for the studied test system in all the areas. In this test system, the WTG is connected to area-1,
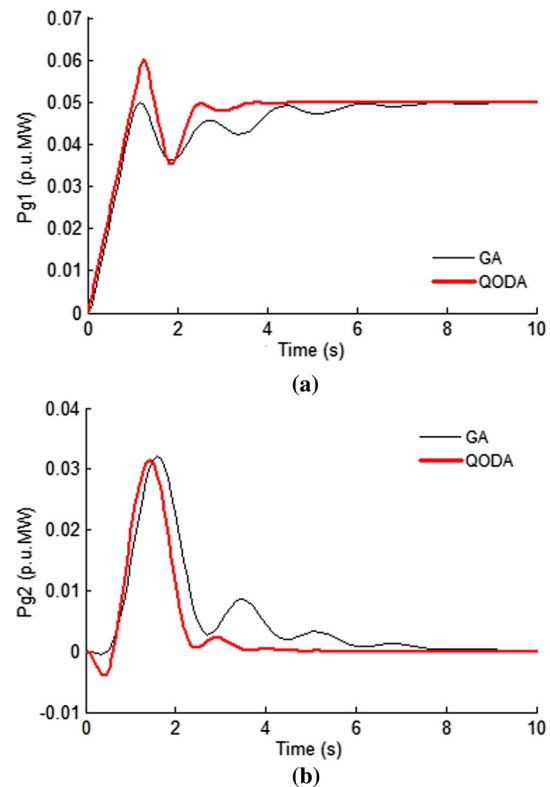

Fig. 7 Comparative output powers of synchronous generators of the studied two-area test system subjected to SLP applied in area-1: **a** ΔP_{g1} and **b** ΔP_{g2}

Table 3 Optimized PID controller gains subjected to multiple SLP for three-area test system (refer Scenario II)

Control area	QODA-PID			QODA-PID-RES			GA-PID-RES		
	K_p (-ve)	K_i (-ve)	K_d (-ve)	K_p (-ve)	K_i (-ve)	K_d (-ve)	K_p (-ve)	K_i (-ve)	K_d (-ve)
Area-1	0.1668	0.3854	0.3965	0.3406	0.1501	0.5380	0.2078	0.3717	0.8907
Area-2	0.5620	0.0584	0.6103	0.0541	0.1147	0.5380	0.9298	0.2547	0.9727
Area-3	0.3913	0.0010	0.0010	0.2444	0.0286	0.0644	0.2195	0.0869	0.0127

(a)

(b)

(c)

(d)

(e)

(f)

Fig. 8 continued

Fig. 8 Comparative dynamic response profiles offered by the studied three-area test system subjected to SLP applied in area-1: **a** Δf_1, **b** Δf_2, **c** Δf_3, **d** $\Delta P_{\text{tie}12}$, **e** $\Delta P_{\text{tie}23}$ and **f** $\Delta P_{\text{tie}31}$
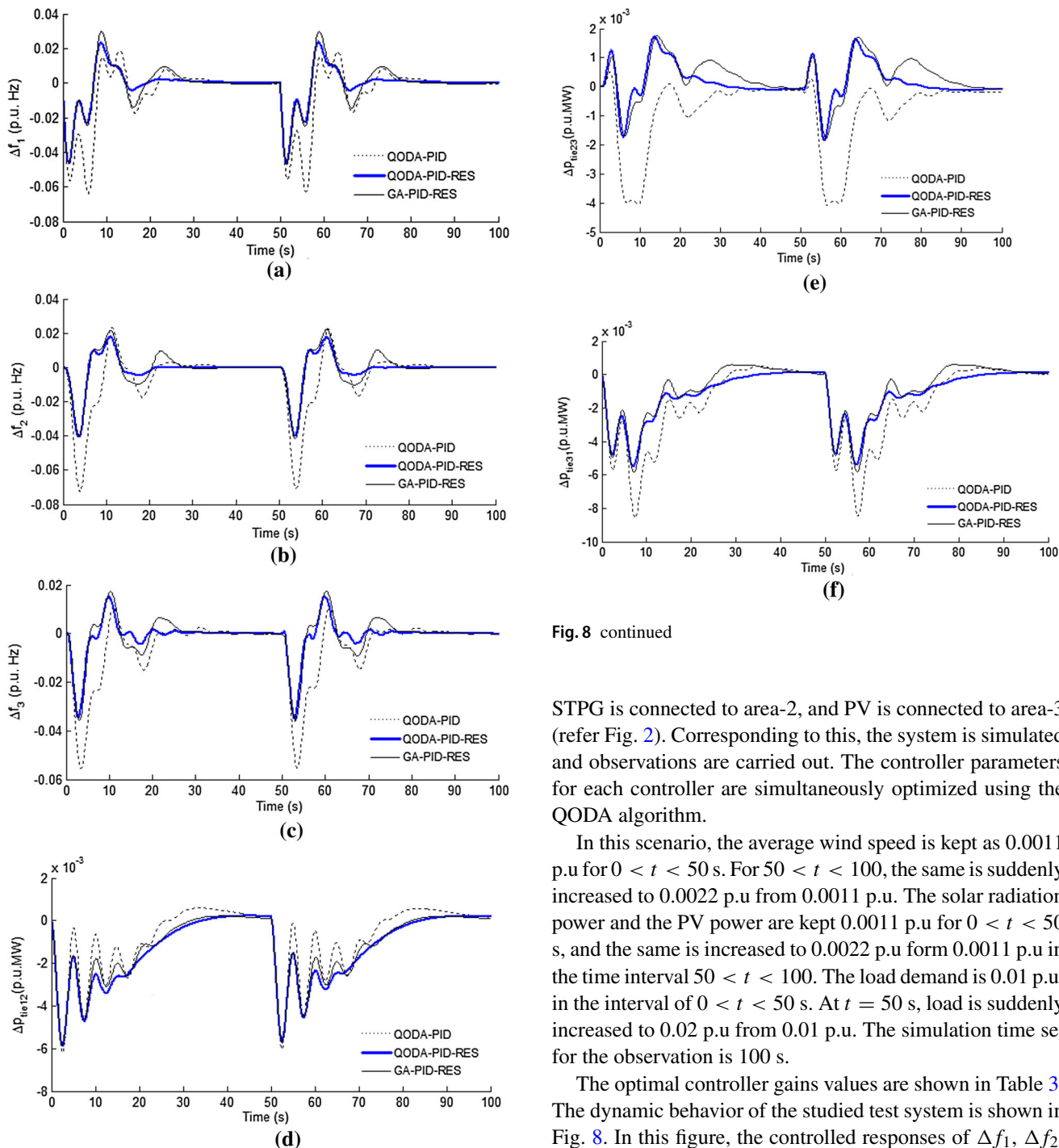
STPG is connected to area-2, and PV is connected to area-3 (refer Fig. 2). Corresponding to this, the system is simulated and observations are carried out. The controller parameters for each controller are simultaneously optimized using the QODA algorithm.

In this scenario, the average wind speed is kept as 0.0011 p.u for $0 < t < 50$ s. For $50 < t < 100$, the same is suddenly increased to 0.0022 p.u from 0.0011 p.u. The solar radiation power and the PV power are kept 0.0011 p.u for $0 < t < 50$ s, and the same is increased to 0.0022 p.u form 0.0011 p.u in the time interval $50 < t < 100$. The load demand is 0.01 p.u. in the interval of $0 < t < 50$ s. At $t = 50$ s, load is suddenly increased to 0.02 p.u from 0.01 p.u. The simulation time set for the observation is 100 s.

The optimal controller gains values are shown in Table 3. The dynamic behavior of the studied test system is shown in Fig. 8. In this figure, the controlled responses of Δf_1, Δf_2, Δf_3, $\Delta P_{\text{tie}12}$, $\Delta P_{\text{tie}23}$ and $\Delta P_{\text{tie}31}$ for the explored control techniques are shown. From this curve, it is quite easy to distinguish that the QODA-PID controller offers oscillations in

Table 4 Comparative ITAE and performance indices values subjected to multiple SLP for three-area test system (refer Scenario II)

Studied controller types	Objective function	Performance indices		
	ITAE	IAE	ITSE	ISE
QODA-PID [studied]	102.83	3.0176	2.6339	0.0886
GA-PID-RES [studied]	77.1071	2.1303	1.1356	0.0353
QODA-PID-RES [proposed]	**53.4219**	**1.6114**	**0.8160**	**0.0277**
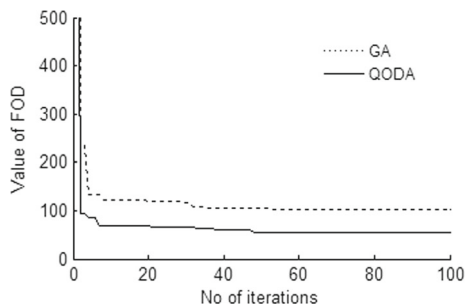
Fig. 9 Comparative convergence plot of ITAE value pertaining to scenario (II)

the system without RESs. When GA-PID-RES-based control technique is applied on the system, the dynamic performance of the system has been enhanced. The GA-based responses have been improved further with the application of QODA technique. The results showed that QODA-PID-RES-based control method is better than GA-PID-RES one. It may be justified by lower ITAE value and other three performance indices values (refer Table 4). Furthermore, the dynamic responses also show that power generation from thermal systems and hydrogeneration of respective areas is fully reached to its steady-state value to maintain the power balance in each area.

The convergence profile of ITAE value with the iteration cycle is also shown. Comparative convergence mobility as obtained by the proposed QODA algorithm and the studied GA is plotted in Fig. 9. This figure shows the better convergence characteristics for the QODA technique. The point is that the proposed QODA works better in the optimal tuning of the PID gains. That's why better dynamic responses have been observed with the QODA technique.

5.3 Scenario (III): Dynamic Responses of Three-Area Power System Model with Random SLP

The same three-area power system model has been taken in this case for the random load perturbation (refer Fig. 5c), and the same is applied in area-1. In this case, the effects of wind energy generations are taken into account for the LFC study. In this test system, only WTG is connected to area-1 (refer Fig. 3). The optimized PID controller gains with and without WTG for the applied load perturbation are shown in Table 5. The system dynamic responses are shown in Fig. 10. The observations reveal that PID controller with WTG shows stable performance in terms of damping oscillations, overshoots and undershoots. The simulation results show that WTG may be used as the primary control of frequency.

6 Conclusion

The present study has showed the RES integration-based LFC approach to the conventional power system model. The RESs has been employed to support the LFC loop along with the conventional generating units. Initially, it has been demonstrated that QODA algorithm is a better optimization technique as compared to both conventional and non-conventional ways of optimization techniques with the help of two-area power system model. After this, the interconnected three-area hydrothermal power system model has been taken to demonstrate the impacts of RESs. The proposed control strategy is QODA algorithm and has been applied to tune the PID controller parameters in the presence of RESs for the better secondary control action.
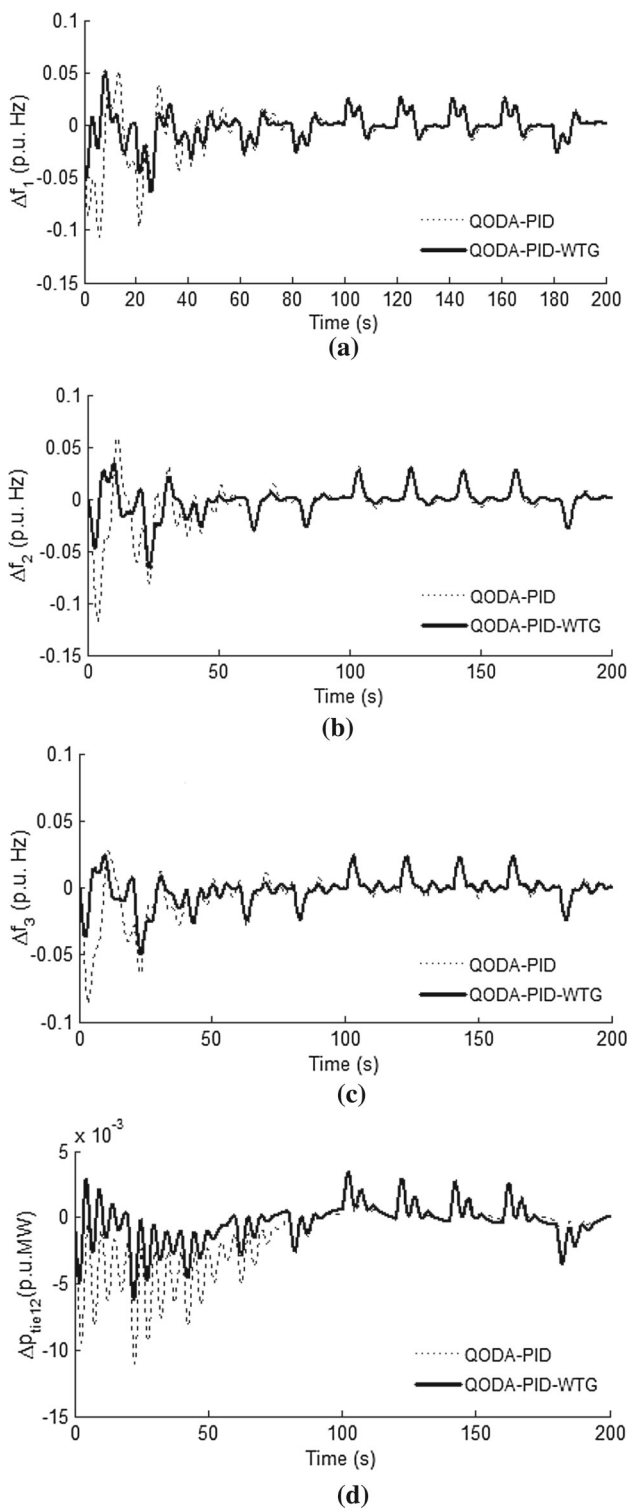
Table 5 QODA optimized PID controller gains subjected to random SLP for three-area test system with WTG (refer Scenario III)

Control area	QODA-PID			QODA-PID-WTG		
	K_p (-ve)	K_i (-ve)	K_d (-ve)	K_p (-ve)	K_i (-ve)	K_d (-ve)
Area-1	0.9875	0.6935	0.5455	0.4840	0.7675	0.7968
Area-2	0.0020	0.0470	0.1355	0.4987	0.3415	0.4088
Area-3	0.5097	0.0031	0.0054	0.3942	0.0083	0.0233

Fig. 10 Comparative dynamic response profiles of the studied three-area power system model subjected to random SLP applied in area-1: **a** Δf_1, **b** Δf_2, **c** Δf_3, **d** $\Delta P_{\text{tie}12}$, **e** $\Delta P_{\text{tie}23}$, and **f** $\Delta P_{\text{tie}31}$

Fig. 10 continued

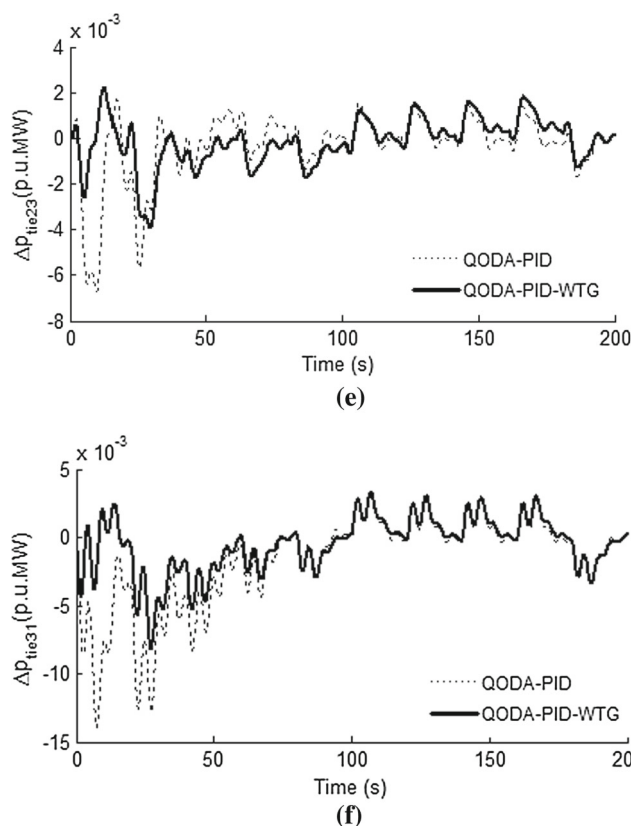A comparative study of LFC performance of the proposed QODA method with GA and conventional way of tuning PID controller has been performed. The LFC responses have been analyzed with and without integrating RESs in three-area power system model. The simulation results showed that QODA is a better optimization technique for the LFC problem. The point of observations of this study is as follows.

(a) The tuning efficiency of QODA algorithm is better than both the non-conventional GA and the conventional way of tuning the PID controllers, i.e., ZN method.
(b) The QODA algorithm is effective to find the optimal gains of PID controller with the presence of RESs.
(c) The RESs may be used as the primary frequency control task in the interconnected power system.

As RES capacity and instantaneous penetration increase in the future, this phenomenon will become more pronounced. Hence, the controller has either to be designed for all credible dispatch scenarios and at least all N-1 contingencies or it has to be re-programmed in time at least whenever the open loop transfers function in each area changes significantly. This can be the extended research works that need to be done ahead.

Compliance with Ethical Standards

Conflict of interest The authors have declared that no competing interests exist and have no conflicts of interest.

Appendix

Nominal Parameters of Two-Area System with Non-reheat Turbine (Shiva et al. 2015).

$P_r = 2000$ MW(rating); $f_{sys} = 60$ Hz; $B_1 = B_2 = 0.425$ p.u.MW/Hz; $R_1 = R_2 = 2.4$ Hz/p.u; $T_{g1} = T_{g2} = 0.03$ s; $T_{t1} = T_{t2} = 0.3$ s; $K_{p1} = K_{p2} = 120$ Hz/p.u.MW; $T_{p1} = T_{p2} = 20$ s; $T_{12} = 0.545$ p.u; $a_1 = a_2 = -1$.

Nominal Parameters of Unequal Three-area Hydro-Thermal Power System (Shiva and Mukherjee 2015)

$f_{sys} = 60$ Hz; $R_{th} = R_h = 2.4$ Hz/p.u; $T_{g_1} = T_{g_2} = 0.08$ s; $\Delta P_{tie\,max} = 200$ p.u.MW; $T_{r_1} = T_{r_2} = 10$ s; $K_{r_1} = K_{r_2} = 0.5$; $H_1 = H_2 = H_3 = 5$ s; $B_1 = B_2 = B_3 = 0.425$ p.u.MW/Hz; $P_{r_1} = P_{r_2} = P_{r_3} = 2000$ MW; $T_{t_1} = T_{t_2} = 0.3$ s; $K_{pe} = 1$; $K_{de} = 4$; $K_{ie} = 5$; $T_w = 1$ s; $T_r = 5$ s; $K_{ps_1} = K_{ps_2} = K_{ps_3} = 120$ Hz/p.u.MW; $T_{ps_1} = T_{ps_2} = T_{ps_3} = 20$ s; $D_1 = D_2 = D_3 = 8.33 \times 10^{-3}$ p.u.MW/Hz; $T_{12} = T_{23} = T_{31} = 0.086$ p.u.MW/rad; $a_{12} = a_{23} = a_{31} = -1$.

Parameters of GA

Number of parameters depends on problem variables (AGC configuration), number of bits = (number of parameters)*8, population size = 50, maximum number of iteration cycles = 100, mutation rate = 0.04, crossover rate = 80%.

Parameters of QODA (Mirjalili 2016)

Number of parameters depends on problem variables (LFC configuration), population size = 50, maximum number of iteration cycle $(\max_{\rm iter}) = 100$, $e = 0.1 \times \left(1 - \frac{2 \times iter}{\max\_iter}\right)$, $s = a = c = 2 \times rand * e$, $f = 2 \times rand$, and $w = 0.9 - \frac{0.5 \times iter}{\max\_iter}$.

References

Ali, E. S., & Abd-Elazim, S. M. (2013). BFOA based design of PID controller for two area load frequency control with nonlinearities. *International Journal of Electrical Power and Energy Systems, 51*, 224–231. https://doi.org/10.1016/j.ijepes.2013.02.030.

Aziz, A., Oo, A. T., & Stojcevski, A. (2018). Analysis of frequency sensitive wind plant penetration effect on load frequency control of hybrid power system. *International Journal of Electrical Power and Energy Systems, 99*, 603–617. https://doi.org/10.1016/j.ijepes.2018.01.045.

Bevrani, H., Ghosh, A., & Ledwich, G. (2010). Renewable energy sources and frequency regulation: Survey and new perspectives. *IET Renewable Power Generation, 4*(5), 438–457. https://doi.org/10.1049/iet-rpg.2009.0049.

Das, D. C., Roy, A. K., & Sinha, N. (2012). GA based frequency controller for solar thermal-diesel-wind hybrid energy generation/energy storage system. *International Journal of Electrical Power and Energy Systems, 43*(1), 262–279. https://doi.org/10.1016/j.ijepes.2012.05.025.

Farahani, M., Ganjefar, S., & Alizadeh, M. (2012). PID controller adjustment using chaotic optimisation algorithm for multi-area load frequency control. *IET Control Theory and Applications, 6*(13), 1984–1992. https://doi.org/10.1049/iet-cta.2011.0405.

Guha, D., Roy, P., & Banerjee, S. (2017). Quasi-oppositional symbiotic organism search algorithm applied to load frequency control. *Swarm and Evolutionary Computation, 43*, 46–67. https://doi.org/10.1016/j.swevo.2016.10.001.

Karavas, C. S., Kyriakarakos, G., Arvanitis, K. G., & Papadakis, G. (2015). A multi-agent decentralized energy management system based on distributed intelligence for the design and control of autonomous polygeneration microgrids. *Energy Conversion and Management, 103*, 166–179. https://doi.org/10.1016/j.enconman.2015.06.021.

Kouba, N. E. Y., Menaa, M., Hasni, M., & Boudour, M. (2016). LFC enhancement concerning large wind power integration using new optimised PID controller and RFBs. *IET Generation, Transmission and Distribution, 10*(16), 4065–4077. https://doi.org/10.1049/iet-gtd.2016.0385.

Lee, D. J., & Wang, L. (2008). Small-signal stability analysis of an autonomous hybrid renewable energy power generation/energy storage system part I: Time-domain simulations. *IEEE Transactions on Energy Conversion, 23*(1), 311–320. https://doi.org/10.1109/TEC.2007.914309.

Luo, C., Far, H. G., Banakar, H., Keung, P. K., & Ooi, B. T. (2007). Estimation of wind penetration as limited by frequency deviation. *IEEE Transactions on Energy Conversion, 22*(3), 783–791. https://doi.org/10.1109/TEC.2006.881082.

Mauricio, J. M., Marano, A., Gómez-Expósito, A., & Ramos, J. L. M. (2009). Frequency regulation contribution through variable-speed wind energy conversion systems. *IEEE Transactions on Power Systems, 24*(1), 173–180. https://doi.org/10.1109/TPWRS.2008.2009398.

Meraihi, Y., Ramdane-Cherif, A., Acheli, D., & Mahseur, M. (2020). Dragonfly algorithm: A comprehensive review and applications. *Neural Computing and Applications.* https://doi.org/10.1007/s00521-020-04866-y.

Mirjalili, S. (2016). Dragonfly algorithm: a new meta-heuristic optimization technique for solving single-objective, discrete, and multi-objective problems. *Neural Computing and Applications, 27*, 1053–1073. https://doi.org/10.1007/s00521-015-1920-1.

Modi, N., Khare, M., & Chaturvedi, K. (2013). Performance analysis of load frequency control in single area power system using GA and PSO based PID controller. *International journal of electrical, electronics and computer engineering, 2*(1), 108–114.

Morren, J., de Haan, S. W. H., Kling, W. L., & Ferreira, J. A. (2006). Wind turbines emulating inertia and supporting primary frequency control. *IEEE Transactions on Power Systems, 21*(1), 433–434. https://doi.org/10.1109/TPWRS.2005.861956.

Muhssin, M. T., Cipcigan, L. M., Obaid, Z. A., & AL-Ansari, W. F., (2017). A novel adaptive deadbeat- based control for load frequency control of low inertia system in interconnected zones north and south of Scotland. *International Journal of Electrical Power and Energy Systems, 89*, 52–61. https://doi.org/10.1016/j.ijepes.2016.12.005.

Nandi, M., Shiva, C. K., & Mukherjee, V. (2017). TCSC based automatic generation control of deregulated power system using quasi-oppositional harmony search algorithm. *Engineering Science and Technology, an International Journal, 20*(4), 1380–1395. https://doi.org/10.1016/j.jestch.2016.08.021.

Nayeripour, M., Hoseintabar, M., & Niknam, T. (2011). Frequency deviation control by coordination control of FC and double-layer capacitor in an autonomous hybrid renewable energy power generation system. *Renewable Energy, 36*(6), 1741–1746. https://doi.org/10.1016/j.renene.2010.12.012.

Pal, P., & Dey, R. (2015). Optimal PID controller design for speed control of a separately excited DC motor: A firefly based optimization approach. *The International Journal of Soft Computing, Mathematics and Control, 4*(4), 39–48.

Pan, I., & Das, S. (2015). Fractional order fuzzy control of hybrid power system with renewable generation using chaotic PSO. *ISA Transactions, 62*, 19–29. https://doi.org/10.1016/j.isatra.2015.03.003.

Rahman, A., Saikia, L. C., & Sinha, N. (2016). AGC of dish-Stirling solar thermal integrated thermal system with biogeography based optimised three degree of freedom PID controller. *IET Renewable Power Generation, 10*(8), 1161–1170. https://doi.org/10.1049/iet-rpg.2015.0474.

Rahman, C. M., & Rashid, T. A. (2019). Dragonfly algorithm and its applications in applied science survey. *Computational Intelligence and Neuroscience, 2019*, 1–21. https://doi.org/10.1155/2019/9293617.

Rahnamayan, S., Tizhoosh, H. R., & Salama, M. M. A. (2008). Opposition versus randomness in soft computing techniques. *Applied Soft Computing Journal, 8*(2), 906–918. https://doi.org/10.1016/j.asoc.2007.07.010.

Reynolds, C. W. (1987). Flocks, herds, and schools: A distributed behavioral model. *Computer Graphics (ACM), 14*, 25–34. https://doi.org/10.1145/37402.37406.

Rosas, P. (2004). *Dynamic influences of wind power on the power system*. Technical University of Denmark.

Shabani, H., Vahidi, B., & Ebrahimpour, M. (2013). A robust PID controller based on imperialist competitive algorithm for load-frequency control of power systems. *ISA Transactions, 52*(1), 88–95. https://doi.org/10.1016/j.isatra.2012.09.008.

Shankar, G., & Mukherjee, V. (2016). Load frequency control of an autonomous hybrid power system by quasi-oppositional harmony search algorithm. *International Journal of Electrical Power and Energy Systems, 78*, 715–734. https://doi.org/10.1016/j.ijepes.2015.11.091.

Shayeghi, H., Jalili, A., & Shayanfar, H. A. (2007). Robust modified GA based multi-stage fuzzy LFC. *Energy Conversion and Management, 48*(5), 1656–1670. https://doi.org/10.1016/j.enconman.2006.11.010.

Shiva, C. K., & Mukherjee, V. (2015). A novel quasi-oppositional harmony search algorithm for automatic generation control of power system. *Applied Soft Computing, 73*, 787–804. https://doi.org/10.1016/j.asoc.2015.05.054.

Shiva, C. K., Shankar, G., & Mukherjee, V. (2015). Automatic generation control of power system using a novel quasi-oppositional harmony search algorithm. *International Journal of Electrical Power & Energy Systems, 73*, 787–804. https://doi.org/10.1016/j.ijepes.2015.05.048.

Shiva, C. K., & Mukherjee, V. (2016). Automatic generation control of hydropower systems using a novel quasi-oppositional harmony search algorithm. *Electric Power Components and Systems, 44*(13), 1478–1491.

Singh, V. P., Mohanty, S. R., Kishor, N., & Ray, P. K. (2013). Robust H-infinity load frequency control in hybrid distributed generation system. *International Journal of Electrical Power & Energy Systems, 46*, 294–305.

Slootweg, J. G., & Kling, W. L. (2003). The impact of large scale wind power generation on power system oscillations. *Electric Power Systems Research, 67*(1), 9–20. https://doi.org/10.1016/S0378-7796(03)00089-0.

Tavakkoli, M., Adabi, J., Zabihi, S., Godina, R., & Pouresmaeil, E. (2018). Reserve allocation of photovoltaic systems to improve frequency stability in hybrid power systems. *Energies, 11*(10), 2583–2602. https://doi.org/10.3390/en11102583.

Tavakoli, M., Pouresmaeil, E., Adabi, J., Godina, R., & Catalão, J. P. S. (2018). Load-frequency control in a multi-source power system connected to wind farms through multi terminal HVDC systems. *Computers and Operations Research, 96*, 305–315. https://doi.org/10.1016/j.cor.2018.03.002.

Tizhoosh, H. R. (2005). Opposition-based learning: A new scheme for machine intelligence. In *Proceedings—International conference on computational intelligence for modelling, control and automation, CIMCA 2005 and international conference on intelligent agents, web technologies and internet*. https://doi.org/10.1109/cimca.2005.1631345

Torreglosa, J. P., García, P., Fernández, L. M., & Jurado, F. (2014). Hierarchical energy management system for stand-alone hybrid system based on generation costs and cascade control. *Energy Conversion and Management, 77*, 514–526. https://doi.org/10.1016/j.enconman.2013.10.031.

Ullah, N. R., Thiringer, T., & Karlsson, D. (2008). Temporary primary frequency control support by variable speed wind turbines—potential and applications. *IEEE Transactions on Power Systems, 23*(2), 601–612. https://doi.org/10.1109/TPWRS.2008.920076.

Valenciaga, F., & Puleston, P. F. (2005). Supervisor control for a stand-alone hybrid generation system using wind and photovoltaic energy. *IEEE Transactions on Energy Conversion, 20*(2), 398–405. https://doi.org/10.1109/TEC.2005.845524.

Yan, R., Saha, T. K., Modi, N., Masood, N. A., & Mosadeghy, M. (2015). The combined effects of high penetration of wind and PV on power system frequency response. *Applied Energy, 145*, 320–330. https://doi.org/10.1016/j.apenergy.2015.02.044.

Van der Zalm, G. M. (2004). Tuning of PID-type controllers: Literature overview. *DCT rapporten Eindhoven: Technische Universiteit Eindhoven, 2004*, 1–23.